$$\theta_{CB} = \frac{\delta}{5} + \frac{5}{6EI}(50 - 200) = \frac{\delta}{5} - \frac{750}{6EI}$$

$$\theta_{CD} = -\frac{\delta}{10} + \frac{10}{6EI}(200 - 100) = -\frac{\delta}{10} + \frac{1000}{6EI}$$

$$\theta_{DC} = -\frac{\delta}{10} + \frac{10}{6EI}(-100 + 200) = -\frac{\delta}{10} + \frac{1000}{6EI}$$

$$\theta_{DE} = \frac{\Delta}{5} + \frac{5}{6EI}(-200 + 100) = \frac{\Delta}{5} - \frac{500}{6EI}$$

$$\theta_{ED} = \frac{\Delta}{5} + \frac{5}{6EI}(100 - 200) = \frac{\Delta}{5} - \frac{500}{6EI}$$

Third Stage

At point B the structure is still elastic. In order to maintain continuity at B

$$\theta_{BA} = \theta_{BC}$$

Substituting for θ_{BA} and θ_{BC} gives

$$\frac{\Delta}{5} + \frac{1000}{6EI} = \frac{\delta}{5}$$

which is a relationship between the two unknown deflections.

Each hinge in turn must now be assumed to form last.

A forms last. $\theta_{AB} = 0$ fixed support at A, that is

$$\Delta = \frac{1041.7}{EI} \qquad \delta = \frac{1875}{EI}$$

C forms last. $\theta_{CB} = \theta_{CD}$ to maintain continuity at C, that is

$$\frac{\delta}{5} - \frac{750}{6EI} = -\frac{\delta}{10} + \frac{1000}{6EI}$$

$$\delta = \frac{972.2}{EI} \qquad \Delta = \frac{138.9}{EI}$$

D forms last. $\theta_{DC} = \theta_{DE}$ to maintain continuity at D

$$-\frac{\delta}{10} + \frac{1000}{6EI} = \frac{\Delta}{5} - \frac{500}{6EI}$$

substitute for δ to give

$$-\frac{\Delta}{10} - \frac{500}{6EI} + \frac{1000}{6EI} = \frac{\Delta}{5} - \frac{500}{6EI}$$

$$\Delta = \frac{555.6}{EI} \qquad \delta = \frac{1388.9}{EI}$$

E forms last. $\theta_{ED} = 0$ fixed support at E

$$\Delta = \frac{416.7}{EI} \qquad \delta = \frac{1250}{EI}$$

Fourth Stage

The largest displacements occur when the hinge at A forms last. Hence at the point of collapse

$$\Delta = \frac{1041.7}{EI} \qquad \delta = \frac{1875}{EI}$$

This frame was used in chapter 3 to illustrate the gradual formation of plastic hinges. The results of that analysis were obtained by a step-by-step stiffness analysis using a computer. The results of that analysis (figure 3.2) are identical to the ones obtained here.

6.2.4 Sloping Members

Structures with sloping members need careful attention. Figure 6.7 shows a typical pitched portal frame. The problem is that, as with the pitched portal

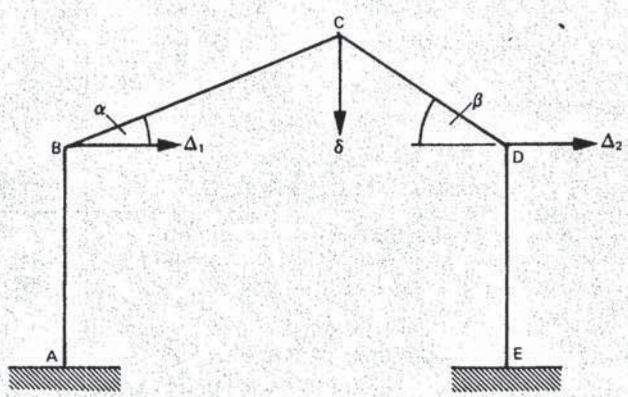

Figure 6.7

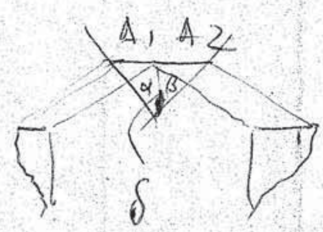

$\tan\alpha = \frac{\Delta_1}{\delta}$ $\tan\beta = \frac{\Delta_2}{\delta}$

$\delta(\tan\alpha + \tan\beta) = \Delta_1 + \Delta_2$

put $\Delta_1 = -\Delta_1$ and (6.3) is <u>OK</u>.

Draw The Compatible State of deformat and from geometry We have

mechanism, the tops of the columns do not deflect the same amount. An extra equation relating these deflections must be found. From the figure

$$\Delta_2 = \Delta_1 + \delta(\tan\alpha + \tan\beta) \tag{6.3}$$

where δ is the vertical deflection at C. Remember that in the slope deflection equations the deflection normal to the sloping members (that is, $\delta \sec\alpha$ and $\delta \sec\beta$) must be used.

6.3 THE EFFECT OF DEFLECTION ON THE COLLAPSE LOAD

The examples in the previous section showed that there can be significant deflections before collapse starts. Deflections, particularly in columns with substantial compressive axial forces, can cause serious instability (buckling) in frames. In this section the effect of this on the collapse load is examined by means of two examples. A practical method of allowing for instability is then outlined.

6.3.1 Horne's Example of a Cantilever Column

Horne [3] has given an excellent illustration of the effect that deflections can have on the collapse load. His example is repeated here in a slightly extended form.

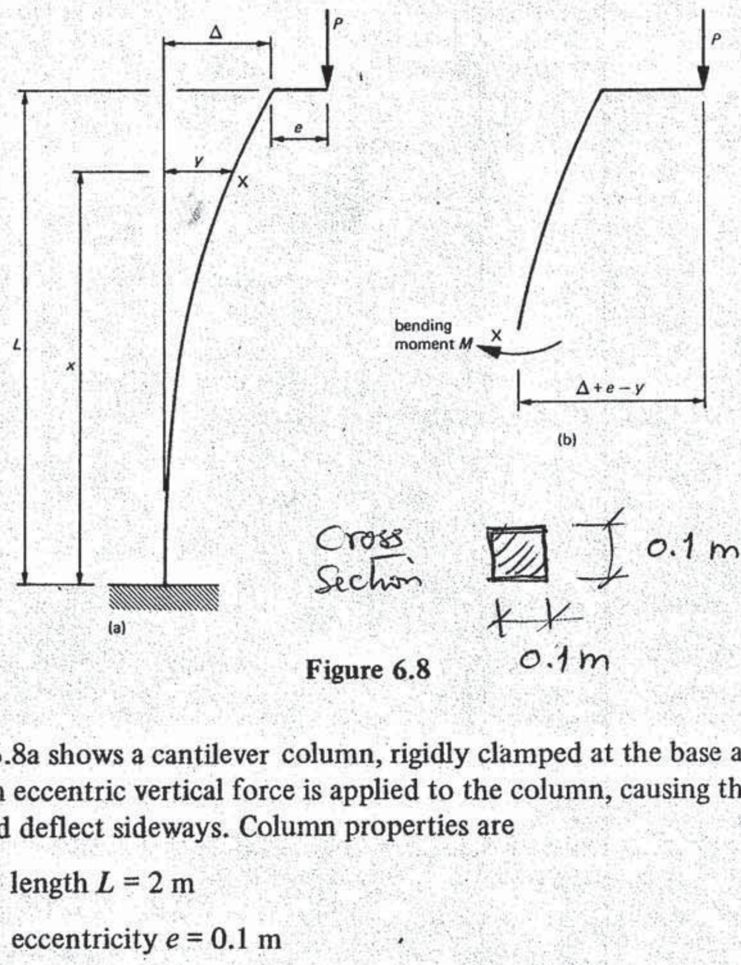

Figure 6.8

Figure 6.8a shows a cantilever column, rigidly clamped at the base and free at the top. An eccentric vertical force is applied to the column, causing the column to bend and deflect sideways. Column properties are

length $L = 2$ m

eccentricity $e = 0.1$ m

Young's modulus $E = 200\ \mathrm{kN/mm^2}$

yield stress $\sigma_y = 250\ \mathrm{N/mm^2}$

Cross-section is square, side length $d = 0.1$ m thus

$$I = \frac{d^4}{12} = 8.333 \times 10^{-6}\ \text{m}^4$$

$$Z = \frac{d^3}{6} = 1.667 \times 10^{-4}\ \text{m}^3$$

$$S\ \text{(plastic modulus)} = \frac{d^3}{4} = 2.5 \times 10^{-4}\ \text{m}^3$$

$$A\ \text{(cross-sectional area)} = \text{d}^2 = 0.01\ \text{m}^2$$

Consider first the elastic behaviour of the column. Figure 6.8b shows the free body diagram from cutting the column at some point X. Moment equilibrium about X gives

$$M = -P(\Delta + e - y)$$

Using the moment curvature relationship of bending theory

$$EI\frac{\text{d}^2y}{\text{d}x^2} = -M = P(\Delta + e - y)$$

which can be rearranged in the form

$$\frac{\text{d}^2y}{\text{d}x^2} + \alpha^2 y = \alpha^2(\Delta + e) \tag{6.4}$$

where $\alpha^2 = P/EI$. This differential equation governs the deflections (y) of the column. The solution of this equation has been shown [15] to be

$$y = (\Delta + e)(1 - \cos \alpha x) \tag{6.5}$$

Substituting $x = L$ and $y = \Delta$ into equation 6.5 gives the deflection Δ at the top of the column

$$\Delta = e(\sec \alpha L - 1)$$

Replacing α and substituting the column properties gives

$$\Delta = 0.1\ [\sec(1.55 \times 10^{-3}\sqrt{P}) - 1] \tag{6.6}$$

0

The load deflection relationship ($P - \Delta$) defined by equation 6.6 is shown in figure 6.9. Although the analysis assumed elastic behaviour the curve is non-linear because of increasing instability in the column. Apparently Δ becomes infinitely large when

$$\sec(1.55 \times 10^{-3}\sqrt{P_E}) = \infty$$

$$1.55 \times 10^{-3}\sqrt{P_E} = \frac{\pi}{2}$$

$$P_E = 1.027 \times 10^6\ \text{N}$$

1

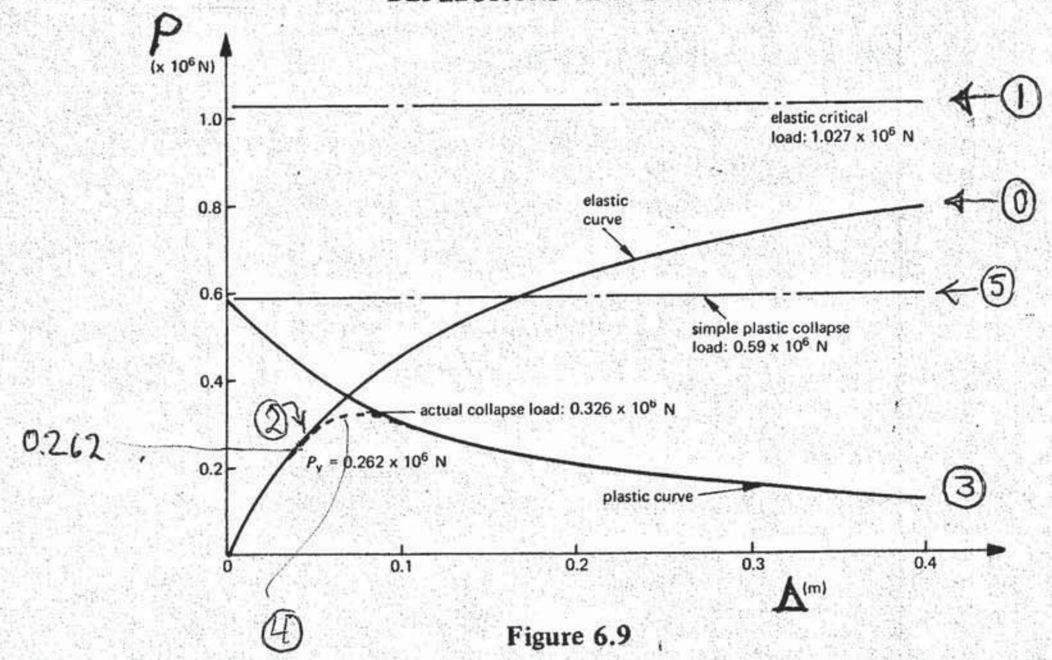

Figure 6.9

It can be shown that when the eccentricity, e, is zero, the strut would remain straight until this load, when it would buckle sideways. P_e is called the *buckling* or *elastic critical* load of the column. 1

The stress in the column is a combination of axial and bending stresses. The largest stress is at the base, where the BM is greatest. When this stress reaches the yield stress the elastic analysis will cease to be correct. This will be when

$$\frac{P}{A} + \frac{P(\Delta + e)}{Z} = \sigma_y$$

substituting for A, Z, Δ, e and σ_y gives

$$100P + 600P \sec (1.55 \times 10^{-3}\sqrt{P}) = 250 \times 10^6$$

This rather complicated equation can be solved by trial and error to show that the load at first yield is

$$P_y = 0.262 \times 10^6 \text{ N}$$ 2

It is possible, but complicated, to trace the spread of yield, but it is more convenient to look now at the collapse of the column. Figure 6.10 shows the collapse mechanism. The column becomes a lever rotating about a plastic hinge at the base. The reduced plastic moment (allowing for the axial force) of the column resists the rotation. From section 2.5

$$\frac{M_p{}'}{M_p} = 1 - \left(\frac{P_c}{P_p}\right)^2$$

Figure 6.10

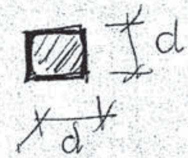

for a rectangular section. Using

$$M_p = S\sigma_y = \frac{d^3\sigma_y}{4}$$

and

$$P_p = A\sigma_y = d^2\sigma_y$$

$$\left(\frac{M_p'}{M_p}\right)+\left(\frac{P_c}{P_p}\right)^2=1$$

and putting $P_c = nP_p$ gives

$$M_p' = (1 - n^2)\cdot\frac{d^3\sigma_y}{4}$$

The moment of the collapse load P_c about the base causes the rotation.

disturbing moment = $(\Delta + e)\,P_c = (\Delta + e)\,nd^2\sigma_y$

At the point of collapse the disturbing and resisting moments are equal, because the column is in equilibrium. At collapse then

$$(\Delta + e)nd^2\sigma_y = (1 - n^2)\frac{d^3\sigma_y}{4}$$

which can be rearranged into

$$n^2 + \frac{4}{d}(\Delta + e)n - 1 = 0$$

The solution of this quadratic equation gives the collapse load P_c as a proportion of P_p, but the solution depends on the deflection Δ at the top of the column. The collapse loads at various values of Δ have been plotted in figure 6.9. (3)

Figure 6.9 summarises the behaviour of the column from zero load until collapse. The broken line shows approximately the transition from elastic behaviour as yield spreads through the base of the column. There are two points to note. (4)

(1) There is substantial deflection before collapse occurs.

(2) A simple plastic collapse calculation would have used the mechanism in figure 6.10 but with $\Delta = 0$. That load (0.590×10^6 N) is considerably greater than the true collapse load (about 0.325×10^6 N). (5)

This is a rather extreme example, but it does illustrate the effects of deflection before collapse. In any frame where there are compressive axial forces in the columns, the true collapse load is smaller than the collapse load predicted by simple plastic analysis. The reduction is usually less marked than shown here (as can be seen in the next example) but cannot be ignored.

6.3.2 Portal Frame Example

A similar analysis for a portal frame is more complicated. The approach is similar to that described in section 3.2 using a stiffness analysis and modifying the structure each time a plastic hinge forms. However, the stiffness matrices for the columns must be formed using the stability functions [14] to allow for the effect of axial load on stiffness. The analysis at each load factor now requires an iterative procedure to arrive at the solution, and is both complicated and expensive in computer time.

portal frame

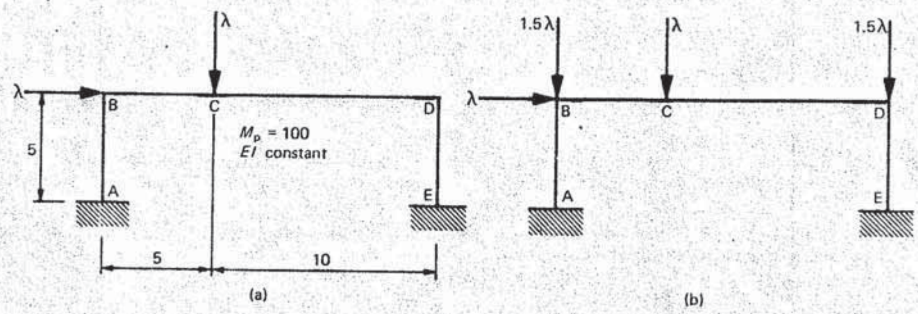

Simulation of Multistorey frame

Figure 6.11

The frame shown in figure 6.11a was analysed in this way and the results are given in figure 6.12. The frame is identical to the one used in sections 3.2 and 6.2.3. In the original analysis (section 3.2), the effects of axial load and deflection were ignored, and the collapse load factor was 50.0. The frame collapsed by the combined mechanism with the hinges forming in the order E, C, D and A. The three load deflection curves in figure 6.12 were obtained by using different EI

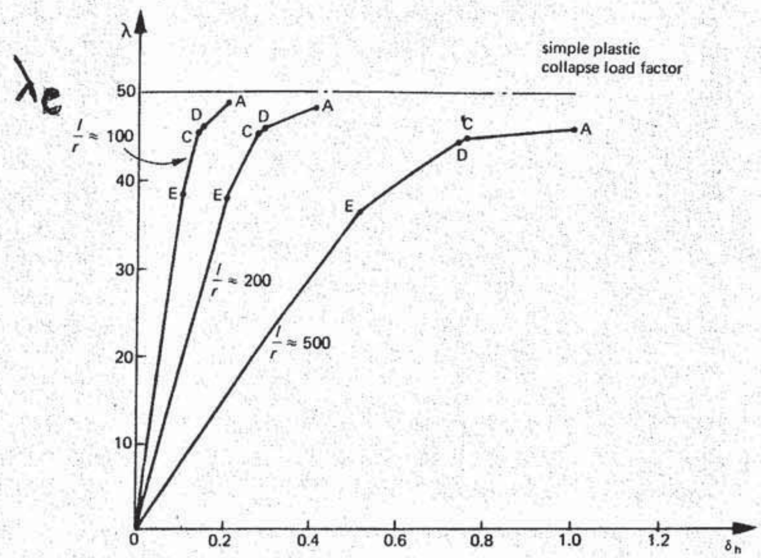

Figure 6.12

values for the members. These were chosen to give slenderness ratios, l/r, for the columns of approximately 100, 200 and 500. The axial loads cause non-linear behaviour between the formation of each plastic hinge, but more importantly, they also reduce the collapse load factor. The bigger the deflections in the structure the bigger the reduction. In each case the final mechanism is the combined one, but in the very flexible frame ($l/r = 500$) the deflections modify the order in which the hinges form. Table 6.2 shows the collapse load factors. The biggest reduction is about 10 per cent although the corresponding l/r ratio of 500 is much greater than would be used in a practical frame. The l/r ratio of 200 is about the practical limit, and in that case, the reduction is about 4 per cent.

Table 6.2

Slenderness ratio (l/r)	100	200	500
Reduced collapse load factor	49.10	48.25	45.93

The reduction in collapse load factor is not really too much of a problem in single-storey frames, but can be much more so in multi-storey frames. Multi-story behaviour has been simulated by applying extra loads to the columns of the portal frame as shown in figure 6.11b. The extra loads represent the weight of the structure and the loading in the higher storeys. As can be seen in figure 6.13 the results are more dramatic. The higher axial loads cause bigger deflections and significant changes in behaviour. Table 6.3 summarises the collapse loads and

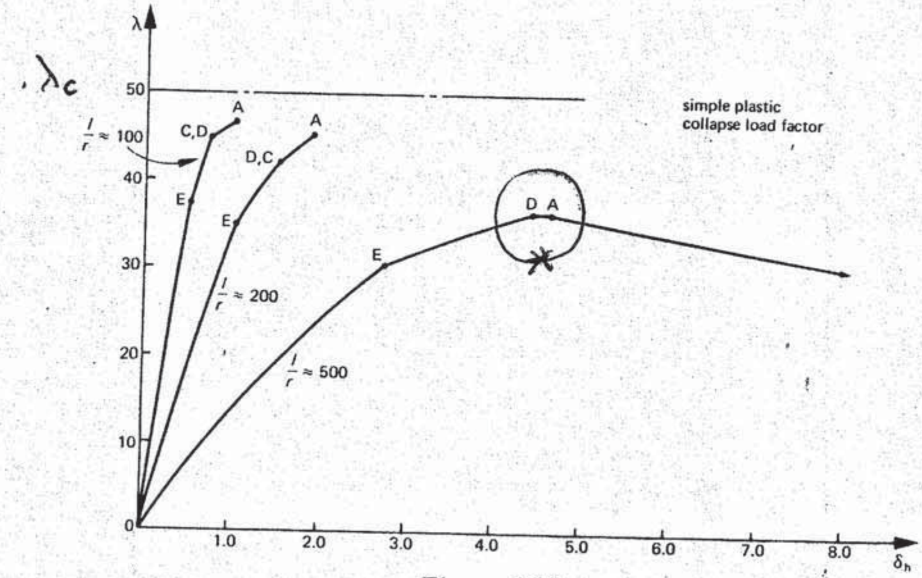

Figure 6.13

mechanisms. (Actually the analysis results are open to question because the deflections are no longer 'small', but the results do give at least a qualitative picture of what can happen.)

Table 6.3

Slenderness ratio	Collapse load factor	Collapse mechanism
100	46.67	Plastic collapse, combined mechanism
200	45.13	Plastic collapse combined mechanism
500	36.60	Sway buckling

In the stiffer frames ($l/r \leqslant 200$) collapse still occurs by the combined mechanism. In the very flexible frame the structure reaches its maximum load before a plastic collapse mechanism forms. In this case the structure becomes unstable when the third hinge forms at A and the structure buckles, as can be seen by the very rapidly increasing deflection.

Wood [16] has explained this type of behaviour. Just as the column in the previous section had an elastic critical load, so too does the frame. (Horne and Merchant [14] have presented a procedure for determining its magnitude.) Usually this load is much greater than the plastic collapse load, as can be seen in table 6.4. However, each time a plastic hinge forms, the stiffness of the frame

After 3 hinges are formed

l/r	Collapse load factor	λ_e modified frame	λ_e original frame	λ_c (simple plastic analysis)	λ_R equation 6.7.
100	49.10	400	2124	50.0	48.9
200	48.25	200	1062	50.0	47.8
500	45.93	80	424	50.0	44.7
100*	46.67	200	531	50.0	45.7
200*	45.13	100	265	50.0	42.1
500*	36.60	7.6	106	50.0	34.0

* Frame loaded as in figure 6.11b

is reduced. The elastic critical load of the frame is now the load for a modified frame with a frictionless hinge at the plastic hinge position. The frame and elastic critical load must be modified successively as each hinge forms. Table 6.4 also shows the elastic critical load of the modified frame when the third plastic hinge has formed. In the case of the flexible frame ($l/r = 500$) that elastic critical load is smaller than the applied load so that buckling must occur.

6.3.3 The Rankine–Merchant Load Factor

The effects of axial force and deflection are rather disturbing. Except perhaps for single-storey frames, it is not enough just to calculate the simple plastic collapse load. It would also be a violation of the elegance and simplicity of the plastic methods to resort to the non-linear computer analysis.

Very stiff structures collapse at the simple plastic collapse load, while very flexible ones buckle at the elastic critical load. In general, these loads can be found without too much difficulty. Merchant devised a means of approximating the true collapse load factor, from the simple plastic collapse and elastic critical loads, based on the Rankine amplification factor used in strut analysis. (The simple plastic collapse load is obtained by the methods described in chapters 3 and 4, which ignore deflections and axial loads.) This approximation, called the *Rankine–Merchant load factor*, λ_R, is defined by the equation

$$\frac{1}{\lambda_R} = \frac{1}{\lambda_c} + \frac{1}{\lambda_e} \tag{6.7}$$

where

λ_c = simple plastic collapse load factor

λ_e = elastic critical load factor

It is plotted in figure 6.14, with the failure loads of several frames tested by Low. The Rankine–Merchant load factor gives in every case a safe approximation of the observed collapse load factor. The Rankine–Merchant load factors for the portal frames in the previous section are given in table 6.3. In every case the Rankine–Merchant approximation is close to, but lower than, the theoretical collapse load factor.

$\frac{\lambda}{\lambda_c}$

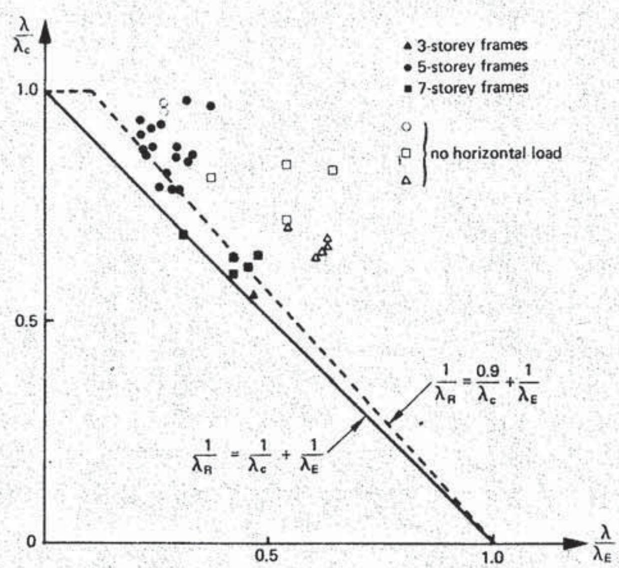

$\frac{\lambda}{\lambda_e}$

Figure 6.14

The apparent conservatism of λ_R as shown in figure 6.14 is partly due to strain hardening during the testing. Wood [17] has suggested the following modification to equation 6.7 to get a better approximation

$$\lambda_R = \lambda_c \qquad \text{when } \frac{\lambda_e}{\lambda_c} > 10$$

$$\frac{1}{\lambda_R} = \frac{0.9}{\lambda_c} + \frac{1}{\lambda_e} \qquad \text{when } 10 > \frac{\lambda_e}{\lambda_c} > 4 \tag{6.8}$$

This is shown by the broken line in figure 6.14. As can be seen, it agrees more closely with the experimental results than the Rankine–Merchant value. When $\lambda_e/\lambda_c < 4$, Wood suggests that the simple analysis is insufficient. It seems likely that Wood's modified equation will be included in the new British code for steel design.

6.4 SUMMARY

This chapter has been concerned with two things: the calculation of deflections at the point of collapse, and the effect that those deflections (and the axial forces) can have on the collapse of the structure.

It was shown initially why it is important in some cases to know the magnitude of deflections before collapse, because limiting those deflections might be more critical than ensuring that the structure is sufficiently strong.

The slope deflection method of calculating these deflections was considered next. The various stages of the procedure are

(1) Determine the collapse mechanism, the corresponding load factor, BMD and end moments (including fixed end moments) of each member of the structure.

(2) Write down the slope deflection equations for each member.

(3) Obtain relationships between the various unknown deflections by considering continuity at every member connection which is shown by the BMD to be elastic. Calculate the deflections, assuming that each plastic hinge in turn is the last one to form.

(4) Choose the last hinge to form and the corresponding set of deflections by using the displacement theorem.

The final part of the chapter was an examination of the non-linear behaviour which results from the axial forces in the members. It was shown that the effect is a reduction in the collapse load factor of the structure, the reduction depending on the stiffness (as measured by slenderness ratio) of the structure: the lower the stiffness, the greater the deflections and reduction in collapse load factor. In single-storey frames the reduction is not usually significant for a structure with practical values of slenderness ratio in the columns. In multi-storey frames the reduction can be more serious, leading to premature buckling before plastic collapse can occur. The Rankine–Merchant load factor was shown to give a good estimate of the reduced collapse load factor, although it appears to be rather conservative when compared to test results. Wood's modification agrees more closely with these results.

6.5 PROBLEMS

6.1 A fixed end beam, span L, carries a vertical load W at a distance $L/3$ from the left hand support. Assuming a constant M_p and EI for the beam determine the vertical deflection at collapse under the load.

6.2 A propped cantilever, span L, carries a UDL w per unit length. Determine the vertical deflection, at collapse, at the plastic hinge near the centre of the span. Assume M_p and EI are constant.